Tuning plasma frequency for improved solar control glazing using mesoporous nanostructures

Geoff B. Smith, Abbas Maaroof, Annette Dowd, Angus Gentle and Michael Cortie
Institute of Nanoscale Technology: University of Technology, Sydney;
PO Box 123, Broadway, NSW 2007 Australia

Keywords: optical properties, conductors, plasma frequency, solar control windows, mesoporous gold, ITO, VO_2

ABSTRACT

The role of the plasma frequency ω_p of conductors in their use for various solar energy and energy efficiency tasks, especially in transparent solar control window coatings, is analysed for a range of materials including noble and other metals, transparent compound conductors and the metallic phase of VO_2. Ways of adjusting ω_p for improved functionality are considered, including novel mesoporous metals and composites that can have an "apparent" or effective plasma frequency. While high ω_p is needed for high thermal infra-red (IR) reflectance and strong surface plasmon resonant absorption, it is not the only requirement. The location of inter-band terms relative to ω_p and the solar infra-red, effective bandwidth, and a high relaxation frequency can each alter these responses substantially. Two materials with elevated carrier relaxation rates, in one case when intrinsic, and in another due to mesostructure, are used to demonstrate this impact. Solar control and visible performance of a mesoporous gold film is analysed.

1. INTRODUCTION

The conductors gold, silver, aluminium, titanium nitride, chromium and indium tin oxide each play important roles as solar energy materials in a variety of special functions which differ according to the topological format of the conductor. Thin films and nanoparticles of the same conductor interact with solar radiation in quite different ways. As a result both formats can provide useful but qualitatively quite distinct spectral selective control, and in film format good electrical conduction may also be possible. The electronic properties which determine each material's complex refractive indices and electrical conductivity, make this spectral selective control possible. Of most importance are carrier density, inter-band transitions that occur at visible and near infra-red (NIR) wavelengths, and carrier relaxation frequencies. Additional excitations associated with charge density waves can arise at conductor surfaces especially if they are non-planar [1], while additional carrier scattering usually occurs in nanostructures [2] due to collisions of electrons with surfaces or defects. High surface–to-volume ratios as in nanoparticles or porous mesostructures, may also influence aspects of inter-band transitions, though in conductors (in contrast to semiconductors), little attention has been paid to this issue to date. We will touch on it using mesoporous gold as an example. This paper will demonstrate that it is important to consider each distinct contribution to dielectric response in developing and evaluating conducting materials for solar applications. Plasma frequency ω_p and hence carrier density, plays the central role and is most easily controlled, but infra red reflection in films, particle absorption strength, and visible transparency if needed depend critically also on relaxation rates and the energy range and strength of interband transitions.

The optics of conductors at long enough wavelengths is often called "plasmonics". It is commonly associated in films with strong, spectrally flat reflectance beyond certain wavelengths. Such conductors which include silver, gold, ITO and aluminium, we will label "strongly plasmonic". However some good electrical conductors we will discuss here can be "weakly plasmonic" in that they do not reflect strongly at long wavelengths as similar thickness thin films, but may still have an almost flat spectral response. They may be stoichiometric materials such as metallic VO_2 or mesostructured metal layers containing noble metals. A complete range of "flat" IR reflectance of conductors at thin film thicknesses of around 12 nm to 18 nm, from strong to weak plasmonics is achievable in mesoporous gold [3]. *This opens up a new approach to achieving a spectrally flat IR reflectance of any desired magnitude.* We will also show that nanoporous

email g.smith@uts.edu.au

Photonics for Solar Energy Systems, edited by Andreas Gombert, Proc. of SPIE Vol. 6197,
61970T, (2006) · 0277-786X/06/$15 · doi: 10.1117/12.661198

conducting gold can have high IR reflectance and hence low emittance, and a change of color. (Color is an important consideration in making solar materials acceptable to users). Mesoporous gold thus behaves like an "effective" or homogeneous metal. We will use this material as an example of how systematic understanding of the way electronic properties and overall optical response are changed by structure can help in choosing and designing the best materials for any spectral control function.

2. PLASMONIC RESPONSE AND SOLAR SPECTRAL CONTROL

The spectral reflectance and transmittance of a 12 nm thick, dense thin film on glass for three important conductors used in solar work are shown in figures 1 and 2. (Each has been modeled to have a common thickness but refractive index data used was that for experimental dense thin film samples). Wavelength is scaled to plasma wavelength $\lambda_p = 2\pi c/\omega_p$ since a basic free carrier model in such a plot would give almost identical curves at frequencies well above the electron relaxation rate (assuming such frequencies are available once the material becomes plasmonic). While there are some common qualitative features in figs. 1 and 2 each plot is quite distinct and for solar applications these differences need to be understood. ω_p for the films in these plots are; 1.9 eV for ITO, 3.3 eV for VO_2 [4] and 8.6 eV for a sputtered gold film. ω_p links to the onset of increased reflectance of good conductors but the λ/λ_p ratios at the turning points in figures 1, 2 range from 1.5 to 3.5, and the long wavelength asymptotic T, R values are clearly quite different. The plasma frequency ω_p depends on the density of free charge carriers n, as $\omega_p^{\,2} = \dfrac{ne^2}{\varepsilon_o m^*}$ with e electronic charge, m* carrier effective mass and ε_o permittivity of free space. These large spectral differences we now link to key electronic properties, which are further modified in nanostructures. The differences apparent in figures 1, 2 for identical thickness films of different conductors translate into even stronger differences for resonant absorption of nanoparticles.

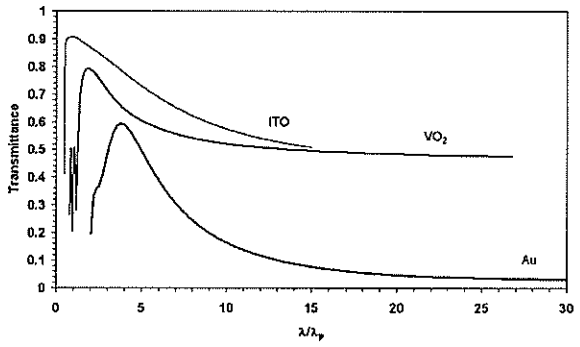

Figure 1. Transmittance as a function of wavelength scaled to plasma wavelength, of 12 nm thick layers of ITO, metallic VO_2, and Au on glass .

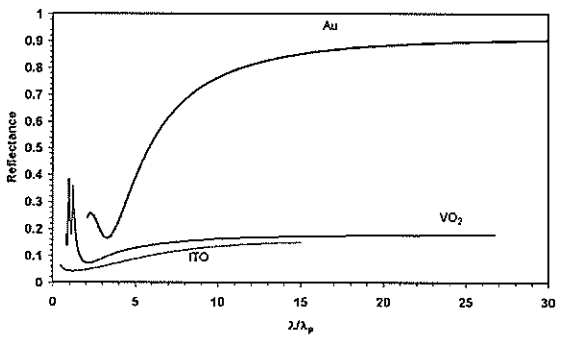

Figure 2. Reflectance as a function of wavelength scaled to plasma wavelength, of 12 nm thick layers of ITO, metallic VO_2, and Au on glass .

2.1 Thin film plasmonic based spectral selectivity

The feature of conducting materials that is most relevant to solar work in figs. 1 and 2, is the transition to a large negative real part of their dielectric constant $\varepsilon(\omega)$, which causes R to rise and T to fall. The free carrier response causes the real part of complex dielectric response $\varepsilon(\omega) = \varepsilon_1(\omega) + i\varepsilon_2(\omega)$ to become negative, but the frequency at which this transition occurs and the sharpness in resultant spectral selectivity as needed for solar functions, is critical and depends not only on ω_p, but on two other features: the lowest energy inter-band contributions and carrier relaxation rates. Equation (1) contains both contributions for the case when visible and NIR/thermal IR properties can be modelled with just one explicit inter-band (ib) oscillator as in gold and silver. [For transparent conductors such as ITO the first and last terms are the same but the interband term is that for a semiconductor and lies in the UV]. The second oscillator is the

Drude or free carrier term which competes with the interband term. This competition must be limited to visible wavelengths to get the desired strong plasmonic response in the solar NIR. In gold and VO_2 ω_p is higher in energy than the lowest energy interband peak centred at $\omega_{j,ib}$. As wavelength increases eventually the Drude term can totally dominate but if the lowest $\omega_{j,ib}$ is also in the NIR (as in the metal phase of VO_2) the onset frequency of useful plasmonics may be too low and also too close to ω_τ, the carrier relaxation rate. It is not often realized that this latter feature also reduces a thin film's ability to be a strong NIR and IR mirror and as a nanoparticle to provide a strong, sharp surface plasmon resonance. Both are desirable for solar applications. These are among the issues currently limiting the performance of VO_2 as a switchable NIR solar control material. It has $\omega_\tau \sim 0.7$ to 1 eV [4] and an interband term near 1 eV and thus strongly exemplifies both weaknesses. Considerable variations in these properties seem to be possible in some recent studies on different VO_2 structures but it remains to be seen how strongly plasmonic its' metal phase can get, given these fundamental restraints. Gold does not have either of these problems. In gold it is the interband and free carrier competition in optical polarisation that leads to low reflectance across half the visible (and some light transmittance in thin films) [5], followed by a rapid rise in reflectance at longer wavelengths to yield a yellow colour. Its spectral selectivity is sharp and quite thin films give very high R values because in the red part of the visible and in the NIR $\omega/\omega_\tau >> 1$ in stark contrast to VO_2.

$$\varepsilon(\omega) = \varepsilon_\infty + \left[\frac{A_{j,ib}}{\omega_{j,ib}^2 - \omega(\omega + i\omega_{\tau,ib})}\right] - \left[\frac{\omega_p^{\,2}}{\omega(\omega + i\omega_\tau)}\right] \qquad (1)$$

ε_∞ is a real number, above 1 due to other higher energy transitions in the UV. $\omega_{\tau,ib}$ gives the effective band-width of the interband term, and $A_{j,ib}$ gives its spectral weight. The relaxation rate ω_τ of mobile electrons in the Drude term can be altered substantially by carrier surface collisions in any nanostructure, but the bandwidth term $\omega_{\tau,ib}$ can also be sensitive to nanostructure. Well into the IR at wavelength ranges where $\omega_j^2/\omega^2 >> 1$, equation (1) can reduce to the simple Drude form of equation (2)

$$\varepsilon(\omega) = \varepsilon_\infty' - \frac{\omega_p^{\,2}}{\omega(\omega + i\omega_\tau)} \qquad (2)$$

ε_∞' is a real constant from combining ε_∞ of equation (1) with the interband term at these wavelengths. It is a good approximation in gold for $\lambda > 2$ μm because gold has $\omega_{j,ib}$ near 3.5 eV (350 nm). Having $\omega_\tau/\omega << 1$ in equation (2) at thermal IR frequencies ensures that a very low thermal emittance arises, even for quite thin films. If ω_τ is larger, as it is in many nanostructures and some conductors, the reflectance plateau in sub-20 nm thick films drops well below values obtainable in dense gold of the same thickness. As a result emittance can rise though it can still be low enough for useful reflection of thermal radiation and hence for thermal insulation in windows, especially if thickness is increased. For example the ω_τ value of ~0.7 eV in thin film VO_2 compared with that in sputtered thin film gold of 0.092 eV means a much lower emittance in thin layers of the same thickness. In gold there is a large gap between the lowest frequency interband term centered at 3.5 eV and the ω_τ at 0.092 eV [6]. (The latter is well clear of the solar NIR). Thus in the solar NIR (0.56 eV $< \omega <$ 2.0 eV) to achieve sharp spectral selectivity and strong IR reflectance (or absorptance in particles) two things are needed in addition to good carrier density. They are (i) ω_j^2/ω^2 large (for the Drude term to dominate) (ii) ω_τ/ω small (to allow a large negative ε_1 to develop). Metallic VO_2 does not satisfy this and is thus weakly plasmonic. Such materials can still be good electrical conductors and are of use as NIR reflectors in thicker layers and for novel applications that exploit other unique properties. We will demonstrate in this paper an approach to controlling key parameters in equation (1) using mesoporosity where the void scale is small enough relative to wavelength not to scatter. In this approach each parameter in equation (1) will become "effective" but they can still be linked back to what is happening inside the conductor. We will show, in practice and in theory, in section 3.1 how structure and level of porosity impact on these effective parameters.

2.2 Factors effecting surface plasmon resonant absorption

The sharpness and strength in resonant response of a conducting nanoparticle in the visible or NIR requires much the same criteria as were just discussed for a strong reflector. This means the combination of electronic parameters in equation (1) must allow the fall of $\varepsilon_1(\omega)$ below zero to be rapid as wavelength increases, so it can quickly attain large negative values. Because we are generalising to arbitrary plasmonic materials at NIR and IR wavelengths, which may have high relaxation rates, we will not make the usual assumption $\omega_\tau/\ \omega << 1$. A conducting nanoparticle with depolarisation factor L for the applied field direction (L = 1/3 for a sphere) embedded in a polymer matrix with $\varepsilon = \varepsilon_h$ has a surface plasmon resonance when its polarizability (α) is maximum. If the ib term is approximately constant we can use equation (2) to find the resonant energy ω_{res}, which is the value of ω satisfying

$$\frac{\omega_p^2}{\omega^2 + \omega_\tau^2} = \varepsilon'_\infty + (\frac{1}{L} - 1)\varepsilon_h = K \qquad (3)$$

The strength and sharpness (hence spectral selectivity or Q factor) for resonant absorption is proportional to $Im(\alpha)$ hence to $\frac{\varepsilon_h}{L\varepsilon_2(\omega_{res})}$ at this frequency. K is approximately constant for all conductors of the same shape in the same matrix, with the only variations associated with the conductor itself from the constant ε'_∞. At resonance one thus has the maximum absorption inversely proportional to

$$\varepsilon_2 = \frac{LK}{\varepsilon_h}\left[\frac{\omega_\tau}{\omega_{res}}\right] = \frac{LK}{\varepsilon_h}\frac{\left[\omega_\tau/\omega_p\right]}{\sqrt{(1/K) - (\omega_\tau/\omega_p)^2}} \qquad (4)$$

For a sphere of gold in a polymer with refractive index of n =1.5, one has $\omega_\tau/\ \omega_{res} \sim 0.03$ so it will have a very much sharper resonance than a sphere of VO_2 in polymer, which has $\omega_\tau/\ \omega_{res} \sim 0.5$. In many nanostructures and in some bulk conductors we cannot assume that $\omega_\tau/\ \omega_{res} << 1$ and thus need to consider the whole spectrum of values for this ratio between that for gold and that of quite weakly plasmonic systems in which it may approach 1. In some applications the broad SP resonance resulting from a large $\omega_\tau/\ \omega_{res}$ ratio may be of practical use.

The key issue for solar blocking by particle absorption is the resonance frequency, ω_{res}. Since particle shape and matrix are often pre-determined by preferred manufacturing processes care is needed in choosing the conductor material. If solar NIR blocking is the dominant concern then ω_{res} should be located around 0.9 μm to 1 μm, and a sharp resonance is best for blocking with a minimum concentration of particles. Shorter wavelengths than 0.9 μm , will almost certainly also cause noticeable visible absorption. If high visible transmittance, high colour rendering index, or a visibly clear window are essential ω_{res} may have to be shifted to longer wavelengths than 1 μm unless equation (4) produces a very narrow absorption band. As most of the solar NIR is at $\lambda < 1.3$ μm, solar NIR absorption is then occurring via the tail of the resonance. Thus to maintain the desired level of NIR blocking requires a large raising of the concentration of particles. We have estimated that the best compromise to achieve the combination of a clear window, strong solar blocking, and minimum particle concentration is to have the typical resonance centred at around 1. 2 μm but the exact best location will depend also on resonance width. Conductors currently in use for such windows [7-9] have sphere resonances either well above or below this value (LaB_6 near 0.8 μm, ITO near 2μm), though some shifting can come from other shapes. There is an additional problem using non-spherical shapes. Unless the particles are oriented during production, the absorption spectrum broadens due to an admix of L values creating multiple resonances. Very broad absorption as occurs in metals such as Mo or Cr can make them useful in solar absorber coatings.

Thus for optimizing particle absorption for windows, we need either conducting materials for which spheres resonate between 1 μm and 1.5 μm, or some other means of tuning the plasma frequency. For wider options in NIR reflectance and emittance in planar systems, materials with novel plasmonic responses are needed.

3. ENGINEERING PLASMA FREQUENCY AND RELAXATION RATES

In planar gold and TiN the value of ω_p plus the lowest interband frequency ω_j, put the reflectance ramp in the middle of the visible range, hence their characteristic yellow/gold colours, while for silver and aluminium which are almost colour neutral, it is at or above the high frequency limit of the visible. For compound conductors such as ITO this transition is in the near infra red (NIR) but they are very visibly transparent because the lowest energy inter-band transitions are at UV energies. Changing plasma frequency while ω_j does not change, would allow new colours in films and new NIR and IR responses in films and particles. We will show an example of a new approach to doing this. The approach to engineering plasma frequency until recently has been to create bulk materials with different carrier densities. Alloying or doping as with ITO, ATO [10] and ZnO:Al [11], or stoichiometry shifts as with TiN_{1+x} [12] have provided some ability to tune ω_p. Reported carrier densities and ω_p in thin film ITO also vary over an order of magnitude according to production details [13]. Such variety in ITO would be useful for nanoparticle tuning but in ITO particles so far used it does not seem to vary to the extent found in coatings, though that may change. It is now possible for optical engineering purposes to have plasmonic responses that go beyond what is available from dense conductors. We now turn to those novel methods which promise scope for achieving a wide variety of plasma frequencies and colors.

3.1 Metamaterials with homogeneous plasmonic responses

The idea that composites or meta-materials containing conductors can behave optically like homogeneous plasmonic systems is relatively new and became of interest with the recent rise in activity in metal composites with "effective" negative refractive index at GHz frequencies [14]. Extensions of the idea to the optical domain has been limited to the context of "spoof" surface plasmons (SP) where resonance in arrays of small sub-wavelength holes spanning metal layers make the whole material appear to act like a novel metal since these hole resonances mimic SP as they yield Drude like dispersion of resonant wavevectors parallel to the surface [15]. Our new approach to engineering bulk plasmonic response [3] relies on metamaterials in which the metal component percolates so that the whole structure retains reasonable dc conductivity. It acts optically like a homogeneous unique metal. We show now that mesoporous gold films provide experimental proof of such an "effective" metal response. It is also given a quite general theoretical basis using a generic effective medium model. The latter indicates that other porous metals can also provide engineered plasmonic responses. To observe useful shifts in plasmonic response from that of the parent metal needs the non–metal component to occupy a significant fraction f of the total volume. The example we provide also has good electrical conduction. Our approach concerns the effective wavevectors in the bulk, not surface waves. The wavelength range over which the theoretical proof we provide is applicable is finite and may not exist at all in some weakly plasmonic conductors. However, experimentally it will be indicated that the full "effective" metal model is a good approximation over a much wider range.

An "effective" metal will have a dielectric response like that given by equations (1) or (2). If data is fitted for these meta-materials the "effective" fitting parameters in (1) or (2) will include impacts from the conductor's complex index (n, k), from the structure, from the insulator phase dielectric constant ε_h (ε_h =1 for voids) and fill factor f. An example of such a fit for a mesoporous gold sample is in figure 3, where we also plot for comparison spectral transmittance for a dense thin gold film. A separate fit (not shown) with equation (1) was done to this data to obtain dense sputtered gold parameters for use in the mesoporous modelling that follows. The generic effective medium model of Bergman [16] reduces to the simple and very useful result appearing in equation (5) for effective dielectric constant ε*[3] for insulator-in-metal comosites, in a specific wavelength range. It is an approximation which is accurate as long as ε_1 is a sufficiently large negative number. This will happen when $(\omega_j/\omega)^2 >> 1$ provided also that $\omega_\tau << \omega_j$ to ensure that the fall in ε_1 has a sufficient band in which to develop. Such ω define a range of wavelengths using λ (μm) = 1.24/ω(eV);

for gold from around 2 μm , while for VO_2 a much longer wavelength would be needed. Equation (2) also applies in this range for ε* and ε.

$$\varepsilon^* = A\varepsilon_{metal} + B\varepsilon_h \tag{5}$$

with A and B real numbers represented by a simple infinite series determined only by geometric factors, and thus they are not wavelength dependent. Since A and B are real and independent of wavelength ε* clearly also has a metal like dielectric response. While equation (5) only works well if ε_1 is a sufficiently large negative number the metal mimic idea can hold outside this range by extending beyond equation (2) to include the interband term in equation (1). We do not have a formal proof of this yet, just experimental evidence and will address the resultant "effective" interband term briefly later. We will now show however that having a range over which equation (5) is applicable enables us to learn a lot of important information on key material parameters. The effective plasma frequency from equation (5) is

$$\omega_p^* = \sqrt{A}\omega_p \tag{6}$$

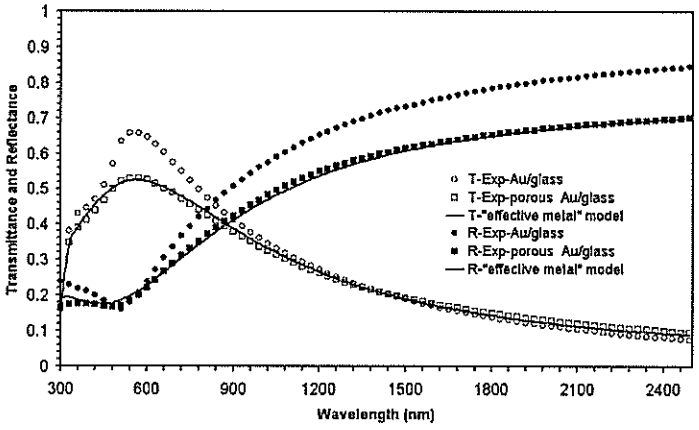

Figure 3. Measured spectral transmittance and reflectance in a mesoporous gold film compared with that of a dense gold film made with the same deposition conditions. Theoretical fits with the "effective" metal model using equation (1) appear as continuous lines while experimental curves are plotted as points.

Hence A is also the effective carrier dilution factor. *Note that A is not simply dilution via the reduced metal density factor of (1-f).* The generic series for A and B reduces to the Maxwell-Garnett model (for void embedded in gold) if only one term is retained in the series, and in this case

$$A = 1 - \left[3f/(2+f)\right] \tag{7}$$

which is less than (1-f), while $B = 9f/(2+f)^2$. Equation (6), using plasma frequencies from fitting data, namely ω_p(dense film-Au) = 8.6 eV and ω_p*(meso-Au film) = 4.5 eV, gives A = 0.47 which from equation (7) gives f = 0.64. We can verify this f value by direct fitting of R and T spectral data with an MG model. Such fitting first requires that the *gold in the mesostructure be assigned correct dielectric constants.* Bulk or dense film data is not appropriate as much increased collision frequency of carriers occurs in such nanostructures. It is also likely (see below) that the interband

term is affected, but we keep that fixed for this paper. If an estimate of the modified or effective ω_τ , which we label ω_τ^* is available, the correction procedure to find ε(Au-in-mesosystem), knowing ε(Au-in-densefilm) and the relaxation rate in the dense film, is straightforward as shown in equation (8).

$$\varepsilon(Au-in-mesosystem) = \varepsilon(Au-densefilm) - \frac{\omega_p^{\,2}}{\omega(\omega + i\omega_\tau^*)} + \frac{\omega_p^{\,2}}{\omega(\omega + i\omega_{\tau,Au-densefilm})} \quad (8)$$

The plasma frequency ω_p is unchanged from that of the dense Au film. Equation (5) provides us with a means to find the effective relaxation rate needed for this correction *directly from measurement* on meso-gold since it requires that $\omega_\tau^* = \omega_\tau(\text{homogenised} - \text{mesoAufilm})$. In other words the "effective" relaxation rate found by fitting data with the "effective metal" model is the *actual relaxation rate in the gold within the mesostructure.* We measured ω_τ* to be 0.29 eV (~ 3x that in dense gold). Applying this corrected gold dielectric constant within the MG model to the sample under study, gives a best fit [3] when f = 0.64. Thus we find exactly the same void content by both routes. This result also validates the idea just presented on how to find actual relaxation frequencies within the metal phase of such systems. In contrast, if we try to fit with a void-in-gold effective medium model without correcting the gold dielectric data first, a good fit is not possible.

3.2 Mesoporous gold as an optically homogeneous metal with plasmonic response

Mesoporous gold has been prepared by a de-alloying etch of sputtered $AuAl_2$ thin films prepared with some ion bombardment during growth. Voids from high resolution SEM studies are typically in the range 15 to 20 nm across with a few at the surface in the range 45 to 60 nm across. A comparison of the transmittance and reflectance spectra for dense gold and mesoporous gold from figure 3 re-plotted in the manner used in Figures 1 and 2 is useful to see that both are clearly plasmonic, but also that the changes in other electronic parameters apart from plasma frequency in the mesoporous sample are having a significant impact. This can be seen from the relatively large shift between curves in figures 4 and 5. The two samples here have different thicknesses to provide similar overall peak visible transmittances. The dense Au film is 10.7 nm thick and the mesoporous Au film with 64% of its volume consisting of voids is 34 nm thick. The plasma wavelength used for the mesoporous film is that from the "effective metal" fit, λ_p = 276 nm, while for the dense gold film it is 144 nm.

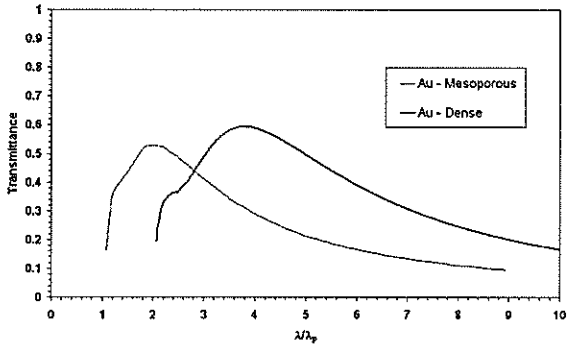

Figure 4. Comparison of spectral transmittance as a function of wavelength scaled to plasma wavelength, of 10.7 nm thick dense Au with that of 34 nm thick meso-Au, both on glass .

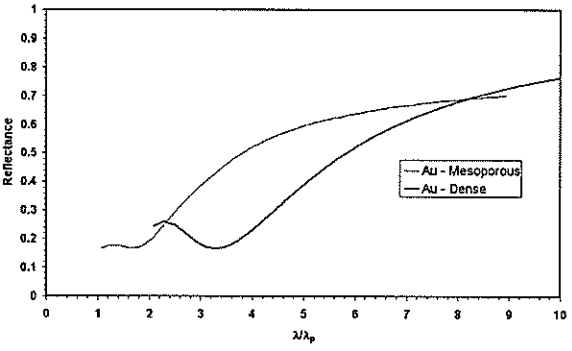

Figure 5 Comparison of spectral reflectance as a function of wavelength scaled to plasma wavelength, of 10.7 nm thick dense Au with that of 34 nm thick meso-Au, both on glass .

The curves have similar shapes but are separated because the relaxation frequency is elevated in the mesoporous film and because its effective plasma frequency is much lower and closer to the mean interband energy than dense gold's plasma frequency. It is interesting that the spectral absorptance A = 1 – R –T from the plots shown for the two sets of curves are similar in magnitude apart from a similar shift along the λ/λ_p axis as shown in Figs 4 and 5 until λ/λ_p is about 7. For longer wavelengths the 34.7 nm thick mesoporous gold has only a small decline in absorptance while in 10.7 nm thick dense gold it continues to decrease to a much higher λ/λ_p ratio. It is this absorptance plateau that defines the thermal emittance which is 0.28 in mesogold, and 0.07 in dense 10.7 nm thick gold film. The long wavelength transmittance values in figure 3 are almost identical but the meso-Au has lower reflectance at these wavelengths. This is attributable to its lower attenuation coefficient k or k* value from the complex indices (n, k) for Au and (n*, k*) for meso-Au, which we have determined at all wavelengths. For example at 2 μm, k ~ 13 while k* is ~ 6, and both k-values rise approximately linearly with wavelength as λ rises in the NIR, as expected for conductors in the plasmonic regime. The slope of k versus λ for meso-Au is much lower than that of dense Au.

A final comment on the effective interband term is needed. From the fitting shown in figure 3 we determined that its centre energy $\omega_{j,ib}$ shifts from 3.5 eV in dense Au to 4.0 in meso-Au. More significant is that the effective bandwidth rises from 1.9 eV in dense-Au to 3.7 eV in meso-Au. This is a significant rise and contributes to the observed neutral color along with the drop in plasma frequency. Its origins are still to be sorted out but seem to be linked both to effective medium impacts and also to changes within the gold. This meso-Au layer is neutral grey in colour due to a combination of the lower (effective) plasma frequency and changes in the interband transitions.

3.2.1 Solar control performance of mesoporous gold thin films

From a perspective of solar heat gain relative to visible light gain both dense and mesoporous gold thin films discussed above give useful spectral selectivity with lower T_{sol} than T_{vis} for each; by around 0.20 in dense gold, and 0.13 in mesogold. Overall performance is as summarized in table 1, where the values presented have been calculated using the Air Mass 1.5 solar spectrum. These table values were found using the spectra in figure 3. The percentage drop in T_{sol} relative to T_{vis} is 31% for dense gold and 25% for the mesogold. The mesogold gives lower T_{sol}, reasonable daylight gain and good clear view, and may be more desirable from a glare perspective. Its solar heat gain coefficient may however be about the same given the additional solar absorptance in mesogold which has A_{sol} of 24%, while the thin gold film has A_{sol} of 13%. Neither of these films has been optimized for a window in a warm climate but give a good idea what is achievable.

Table 1. Solar energy and solar visible light transmittance of 34 nm thick mesoporous gold films on glass compared with 10.7 nm thick dense gold thin films on glass

Samples	T_{VIS}	T_{SOL}	R_{VIS}	R_{SOL}
Dense-Au on glass	0.643	0.447	0.204	0.426
Meso-Au on glass	0.523	0.393	0.199	0.365

4. CONCLUSION

When considering conductors for solar energy materials applications, while the plasma frequency plays the major role in both films and particle performance, both also depend strongly on the frequency of the lowest energy interband terms and the relaxation rate of mobile carriers. Some conductors considered for use in solar work like the metal form of VO_2 were shown to be quite weakly plasmonic with respect to gold. Highly nano-porous gold retains good metal like optical properties. Two approaches to modelling the optical properties of highly mesoporous metals have been established, an "effective metal" model and an effective medium model, which enable effective plasma frequency to be estimated. They have been validated using experimental data. Thus a new approach to tuning plasma frequency has been identified.

5. ACKNOWLEDGEMENTS

We wish to thank Geoff McCredie for help with thin film production, Ric Wuhrer for help with film imaging and characterization, and Gunnar Niklasson of Engineering Science, Uppsala University, Sweden for hospitality during some aspects of this work, and for helpful discussions

REFERENCES

1. H. Raether. "Surface plasmons on smooth and rough surfaces and on gratings", Vol. III of Tracts in Modern Physics (Springer, Berlin, 1988).
2. U. Kreibig and M. Vollner in "Optical properties of metal clusters", Springer Series in Materials Science, Springer-Verlag , Berlin (1995).
3. A. I. Maaroof, M. B. Cortie and G. B. Smith, "Optical properties of mesoporous gold films," *J. Optics A, Pure and Applied Optics* **7**, 303-309 (2005).
4. H.W. Verleur, A.S. Barker, Jr., C.N. Berglund, *"Optical properties of VO_2 between 0.25 and 5 eV", Phys. Rev.*, **172** 788-98 (1968).
5. G.B. Smith, G.A. Niklasson, J.S.E.M. Svensson and C.G. Granqvist, "Noble -metal- based transparent infra-red reflectors: Experiments and Theoretical analyses for very thin gold films", *J. Applied Physics* **59**, 571- 581 (1986).
6. G.B. Smith, A. Maaroof and A. Gentle, "Highly nanoporous conductors as optically homogeneous infra-red mirrors with controllable color" under review *Appl. Phys. Lett.* (available on request)
7. S. Schelm, G.B. Smith, P.D. Garrett and W.K. Fisher, "Tuning the surface plasmon resonance in nanoparticles for glazing applications," *J.Appl. Phys.* **97**, 124314 (1-8) (2005).
8. S. Schelm, G. B. Smith, *"Dilute LaB_6 nanoparticles in polymer as optimised clear solar control glazing", Appl. Phys. Lett.*, **82** 4346-48 (2003).
9. G.B. Smith, C.A. Deller, P.D. Swift, A.Gentle, P.D. Garrett and W.K.Fisher, "Nanoparticle doped polymer foils for use in solar control glazing" , *Journal of Nanoparticle Research*, **Vol. 4/1-2**, 157-165 (2002).
10. B. Stjerna, E.Olsson and C.G. Granqvist, "Optical and electrical properties of radio frequency sputtered tin oxide films doped with oxygen vacancies, F, Sb, or Mo", *J. Applied Physics*, **76**, 3797-3817 (1994).
11. Z.C. Jin, I. Hamberg and C.G. Granqvist, "Reactively sputtered ZnO:Al films for energy-efficient windows", *J. Applied Physics*, **64**, 5117-5131 (1988).
12. G. B. Smith, P. D. Swift and A. Bendavid, "TiNx with metallic behaviour at high N/Ti ratios for better solar control windows", *Applied Physics Letters*, **75**, 630-632 (1999).
13. I. Hamberg and C.G. Granqvist, "Evaporated Sn-doped In_2O_3 films: basic optical properties and applications to energy efficient windows", *J. Applied Physics* **198**, 660, R123 - R159 (1986).
14. J.B. Pendry, A.J. Holden, D.J. Robbins and W.J. Stewart, "Low frequency plasmons in thin wire structures", *J. Phys. : Condens. Matter*, **10**, 4785-4809 (1998).
15. J.B. Pendry. L. Martin-Moreno and F.J. Garcia-Vidal, "Mimicking surface plasmons with structured surfaces", *Science*, **Vol. 305**, 847-848 (2004).
16. D. Bergman, "The dielectric constant of a composite medium-a problem in classical physics", *Physics Reports* **43**, 378 –407 (1978).